

X

## COMETARY DUST

## Composition and Optical Properties of Cometary Dust

Martha S. Hanner

*Jet Propulsion Laboratory, California Institute of Technology,  
Pasadena California 91109*

**Abstract.** Comet dust consists primarily of silicate and carbonaceous material. The carbonaceous material is not yet well-characterized. The 3.36  $\mu\text{m}$  emission feature arises primarily from gas phase molecules, while a small feature at 3.29  $\mu\text{m}$  may be due to aromatic hydrocarbons in the grains. Olivine, a high temperature condensate, is present in some comets. Polarization and albedo maps have shown that the coma is not uniform; an inner halo of large particles may be present.

### Introduction

Comets formed in the outer solar nebula where the temperature remained low enough that interstellar grains could have been incorporated with little alteration. Studies of the solid grains released from comets can help us to understand the conditions in the solar nebula and the extent to which interstellar material was preserved in comets.

Comets apparently originate from two reservoirs in the outer solar system. The comets that populate the inner and outer Oort Cloud probably formed in the Saturn - Neptune region (10 - 30 AU) and were dynamically scattered to the Oort Cloud. This is the source of new and long-period comets. Short-period comets, with their low inclination orbits, most likely originated in the trans-Neptune region at 30 - 100 AU (Duncan *et al.* 1988). The largest objects in this population have now been directly detected (Jewitt & Luu 1995).

If there were compositional gradients in the solar nebula, due to the gradient in temperature or to the extent of mixing between the warm inner regions of the nebula and the comet-forming regions, then one would expect to see differences between the long and short period comets and even within the two populations. Thus, studies of the heterogeneity among comets may lead to a better understanding of how the conditions varied in the solar nebula and the important question of radial transport of material.

No doubt, there are cometary particles among the IDPs collected at Earth and these represent an important resource for studying the processing history of the dust. The anhydrous chondritic aggregate IDPs are the most likely candidates, based on their structure and inferred atmospheric heating (Bradley 1995). However, it is important to verify this identification via independent observations of cometary dust.

The first *in situ* sampling of comet dust composition was obtained by the dust impact analyzer on the Halley probes (Kissel *et al.* 1986). A dust component rich in organic refractory material was discovered, the CHON particles. Usually, C, Si, and Mg occurred together, indicating that the silicate and carbonaceous material were well mixed



on a submicron scale (Jessberger *et al.* 1988). These discoveries provide a framework for interpreting the remote sensing observations. However, the total sample of cometary dust analyzed by these instruments was less than one 10  $\mu\text{m}$  IDP.

In the next decade, the Rosetta mission will visit a comet and the STARDUST mission will return a sample of cometary dust for laboratory analysis. Yet remote sensing remains our best means of surveying the nature of the dust in many comets and comparing with the dust in the interstellar medium. This paper reviews the current status of our knowledge about cometary dust from remote sensing.

## Thermal Emission

The 3.5 - 20  $\mu\text{m}$  spectral energy distribution of the thermal emission from the dust coma gives color temperatures that are 5-25% hotter than that of a theoretical blackbody. Color temperature is determined by the physical temperature of the grains and their wavelength-dependent emissivity. The temperature of a particle in the solar radiation field depends on the balance between the solar energy absorbed at visual wavelengths and the energy radiated in the infrared. Small silicate grains, which are transparent at visual wavelengths, absorb little solar energy yet radiate efficiently at 10  $\mu\text{m}$ . Consequently, they will be cold. Small carbonaceous grains, on the other hand, absorb strongly at visual wavelengths, but cannot radiate efficiently in the infrared at wavelengths greater than about 10 times their size. Thus, they heat up until the energy radiated at 3 - 8  $\mu\text{m}$  balances the absorbed energy. In fact, for small absorbing grains, their size controls the temperature, regardless of the specific composition (Hanner 1983). Grains larger than a few microns will be hotter than a blackbody only if they are very fluffy (e.g. Xing & Hanner 1995).

Thus, we can conclude, independent of a specific model, that the 3-20  $\mu\text{m}$  thermal emission in most active comets arises predominantly from sub- $\mu\text{m}$  to  $\mu\text{m}$  sized absorbing grains. Model calculations of the thermal spectral energy distribution for a size distribution of grains support this conclusion (Hanner 1983; Hanner *et al.* 1985). The comets with the strongest dust emission, such as Halley, have higher color temperature at 3.5 - 8  $\mu\text{m}$  than at 8 - 20  $\mu\text{m}$ , indicating an enhanced abundance of hot, sub- $\mu\text{m}$  grains. Silicates must be sufficiently mixed with absorbing material that they are warm and dark. Only a small imaginary component in the refractive index,  $n'' \geq 0.01$  is actually needed to raise the temperature of micron-sized silicate grains (Hanner 1983); this could be due to finely dispersed carbonaceous material or to the FeNi beads found within the glassy silicate particles described by Bradley (1995).

While the 3 - 20  $\mu\text{m}$  thermal emission allows us to determine the amount of small dust in the coma, these data do not help us determine the amount of mass in large particles, with their lower ratio of cross section to mass. The dust impact detector (DIDSY) on GIOTTO recorded a very broad mass distribution (McDonnell *et al.* 1991). The small slope at masses  $> 10^{-9}$  kg implied that the mass was concentrated in these large particles. Meteor streams associated with comets contain particles in this size range. Radar observations of comets IRAS-Araki-Alcock (Goldstein *et al.* 1984; Harmon *et al.*



1989) and P/Halley (Campbell *et al.* 1989) detected the presence of large grains surrounding the nucleus.

While these particles are "invisible" in the infrared, their thermal radiation may be detectable at longer wavelength, since the emissivity of the small grains will decrease as  $\lambda^{-\alpha}$ ,  $1 \leq \alpha \leq 2$ , while the emissivity of the large grains remains essentially constant. Jewitt and Luu (1990) detected emission from P/Brorsen-Metcalf at 800  $\mu\text{m}$ . If one compares the flux with the 10  $\mu\text{m}$  flux recorded 4 days earlier, one finds that the data are consistent with a radiating blackbody having constant emissivity (Lynch *et al.* 1992a). That is, the large grains emitting at 800  $\mu\text{m}$  can account for the 10  $\mu\text{m}$  flux as well; Brorsen-Metcalf apparently lacked the population of small grains present in most comets, consistent also with the lack of a silicate feature and the low scattered light continuum. In contrast, four other comets measured by Jewitt and Luu (1992) have submillimeter fluxes or upper limits that are one to two orders of magnitude lower than the flux extrapolated from 10  $\mu\text{m}$  on the assumption of constant emissivity.

## Infrared Spectral Features

### *Hydrocarbons*

A broad emission feature centered near 3.36  $\mu\text{m}$  was discovered in the Vega IKS spectra of Halley (Combes *et al.* 1988). The emission is attributed to the stretching vibration of C-H bonds in organic molecules. Subsequent spectra of Halley from ground-based telescopes revealed spectral structure (Fig. 1); the feature persisted to at least 2 AU (Baas *et al.* 1986). A similar emission feature has been detected in every bright comet since Halley, including new, long-period and periodic comets. The strength of the feature correlates with the water production rate, rather than with the continuum brightness, suggesting that the carrier is most likely a gas phase species (Brooke *et al.* 1991).

The narrower emission feature at 3.52  $\mu\text{m}$  has been attributed to the  $\nu^3$  band of methanol, based on the good agreement between the abundance of methanol derived from fitting the infrared feature and that derived from detection of methanol at millimeter wavelengths (Hoban *et al.* 1991). Methanol has other vibrational bands at 3.33  $\mu\text{m}$  ( $\nu^2$ ) and 3.37  $\mu\text{m}$  ( $\nu^9$ ) and these will contribute to the broad 3.36  $\mu\text{m}$  emission (Reuter 1992). Careful modeling of the methanol bands leads to a residual feature centered at 3.424-3.43  $\mu\text{m}$  (Bockelée-Morvan *et al.* 1995; DiSanti *et al.* 1995). The strength of the residual feature correlates with water production rates and especially with the methanol abundance; thus, it is likely to arise from a gaseous species. Assuming a g-factor comparable to that of methanol, the abundance of the carrier is comparable to methanol,  $\sim 4\%$  relative to water, making it a significant reservoir of carbon. Overtone and combination bands of methanol may also contribute. Further progress will require high spectral resolution to resolve line structure and sort out the methanol contribution.

A small, but distinct, feature at 3.29  $\mu\text{m}$  is present in the spectra of the dusty comets Halley (Fig. 1), Levy 1990 XX (Davies *et al.* 1991), and Swift-Tuttle (Di Santi



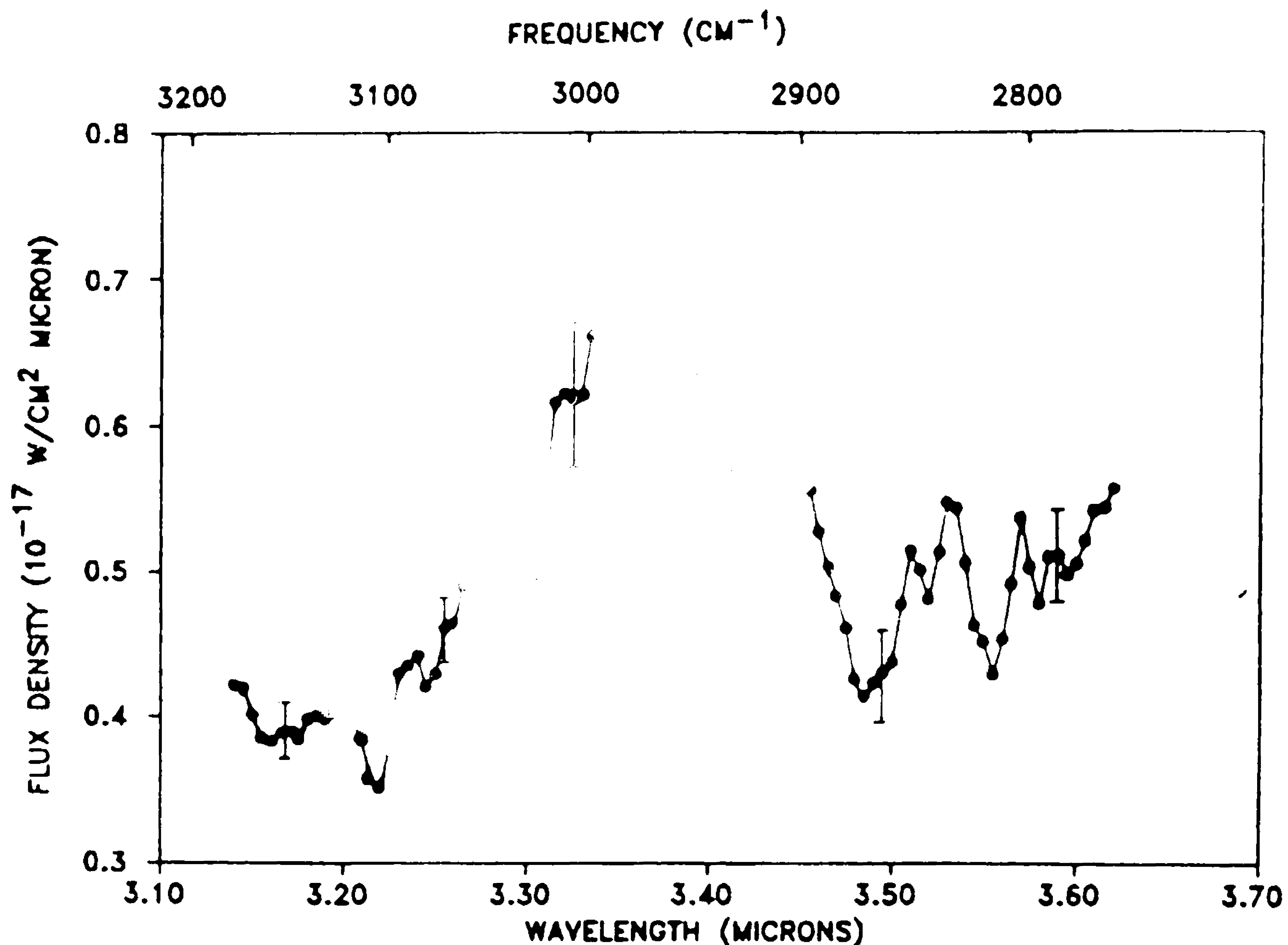


Fig. 1. Spectrum of P/Halley 25 April 1986 at  $R = 1.56$  AU (Baas *et al.* 1986)

*et al.* 1995). In Swift-Tuttle, the feature appeared to be stronger on Nov. 27, when the dust continuum was also stronger. Typical of aromatic bonds, this feature could arise from polycyclic aromatic hydrocarbons either in molecules or small solid grains. An interstellar feature at  $3.29 \mu\text{m}$  is associated with other bands at  $6.2$ ,  $7.7$ ,  $8.6$ , and  $11.3 \mu\text{m}$ . No evidence of the  $6.2$  and  $7.7 \mu\text{m}$  bands is seen in the only  $5\text{--}8 \mu\text{m}$  spectra of comets Halley (Bregman *et al.* 1987) and Wilson 1987 VII (Lynch *et al.* 1989).

Thus, to date, there is no positive identification of a spectral feature from CHON grains, but further study of the  $3.29 \mu\text{m}$  feature is warranted. Indeed, PAHs have been discovered in IDPs (Clemett *et al.* 1993).

### *Silicates*

A silicate emission feature near  $10 \mu\text{m}$  is seen in a number of comets. The shape of the feature can be diagnostic of the silicate mineralogy (e.g. Hanner *et al.* 1994a). Four comets (among the 9 with good spectra) display a strong feature with a peak at  $11.2 \mu\text{m}$  arising from crystalline olivine (Fig. 2). These are long-period comets Bradfield 1987 XXIX (Hanner *et al.* 1990) and Levy 1990 XX (Lynch *et al.* 1992b), new comet Mueller 1993a (Hanner *et al.* 1994b) and P/Halley (Bregman *et al.* 1987; Campins & Ryan 1989).

The olivine identification is based on the good spectral match with the measured spectral emissivity of Mg-rich olivine (Stephens & Russell 1979) and the fact that the peak is seen only in association with a strong silicate feature. Olivine is present in chondritic aggregate IDPs. Other possible materials, such as SiC or hydrocarbons, can be ruled out from the width of the peak, abundance arguments, or for lack of the corresponding features, such as the  $7.7 \mu\text{m}$  and  $8.6 \mu\text{m}$  emission bands present with the  $11.25 \mu\text{m}$  PAH feature in interstellar sources.



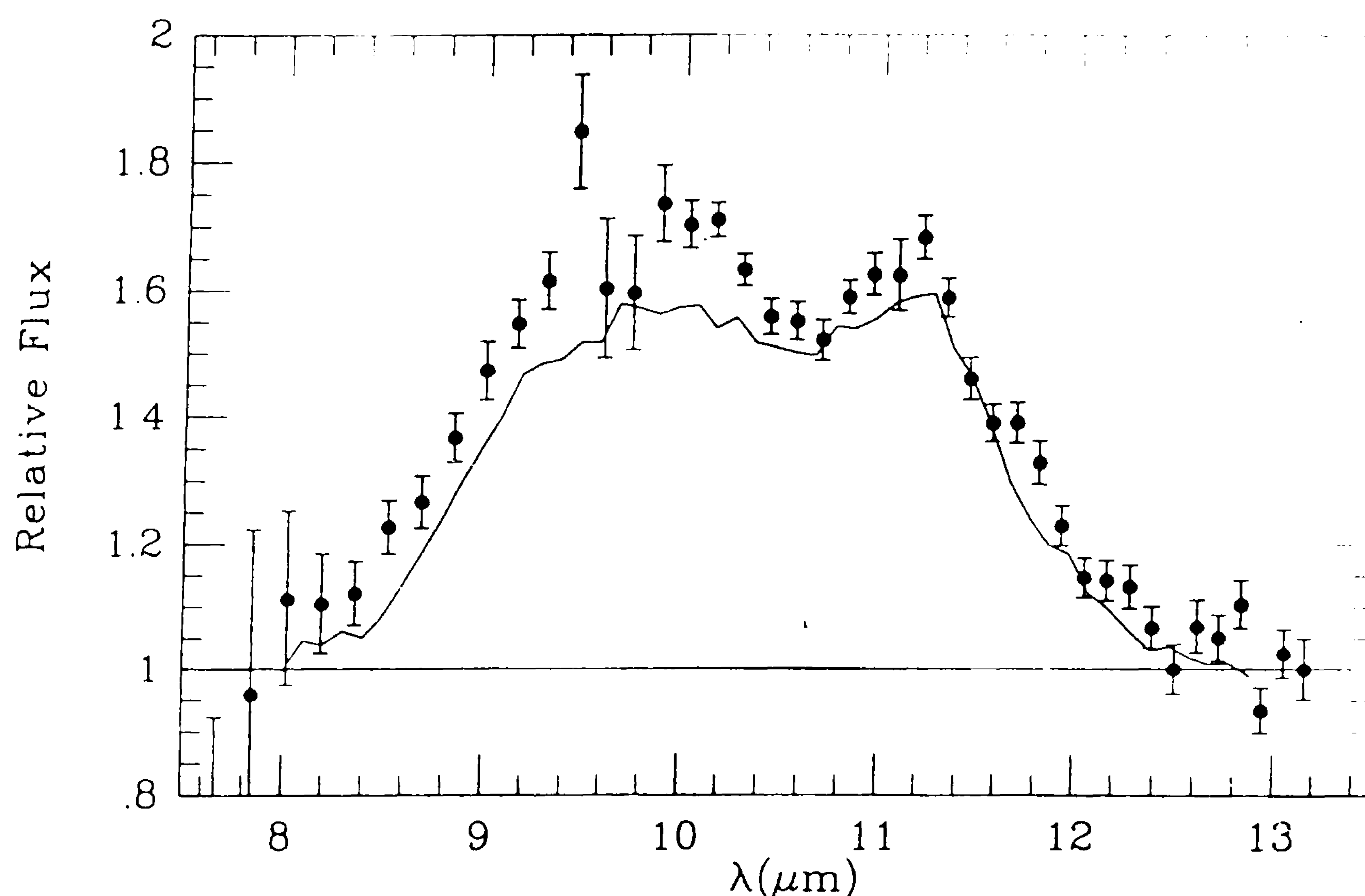


Fig. 2 Silicate feature in Mueller 1993a at  $R = 2.06$  AU (Hanner *et al.* 1994b). Flux divided by 220 K blackbody continuum. Solid line is spectrum of P/Halley at  $R = 0.79$  AU (Campins and Ryan 1989).

This result is significant because olivine is a high-temperature condensate. It can form by direct vapor condensation at  $T \sim 1400$  K followed by slow cooling or by annealing of amorphous silicate grains at  $\sim 900$  K. Such heating did not take place in the outer solar nebula. The spectral signature of olivine is rarely, if ever, seen in the interstellar medium. Thus, its presence in comets may be evidence of the transport of material from the warm inner solar nebula to the region of comet formation. But, so far, the  $11.2 \mu\text{m}$  peak has been seen in only a few comets. A wider sample of cometary spectra - and correlation with other dust properties - are needed to follow up on this potentially important subject.

The broad  $9.8 \mu\text{m}$  maximum in the comet spectra is similar to the interstellar feature and most likely arises from amorphous or glassy particles. Glassy silicate grains are common in chondritic aggregate IDPs. Bradley (1994, 1995) argues that these are, in fact, interstellar grains with significant radiation damage before being incorporated into comets.

The spectra of four other new comets discussed in Hanner *et al.* (1994a) are puzzling; each has a unique, and not understood, spectrum. In Wilson 1987 VII, the feature is extremely broad, suggesting a very amorphous silicate material. We may be witnessing the effect of cosmic ray damage to the outermost layer of the nucleus over the lifetime of the Oort Cloud.

Other comets, such as P/Brosen-Metcalf (Lynch *et al.* 1992a) and many short-period comets lack a silicate feature. The size of the dust grains affects the visibility of the silicate feature. These comets may lack a silicate feature because there is a deficiency of small grains rather than a lack of silicate material.



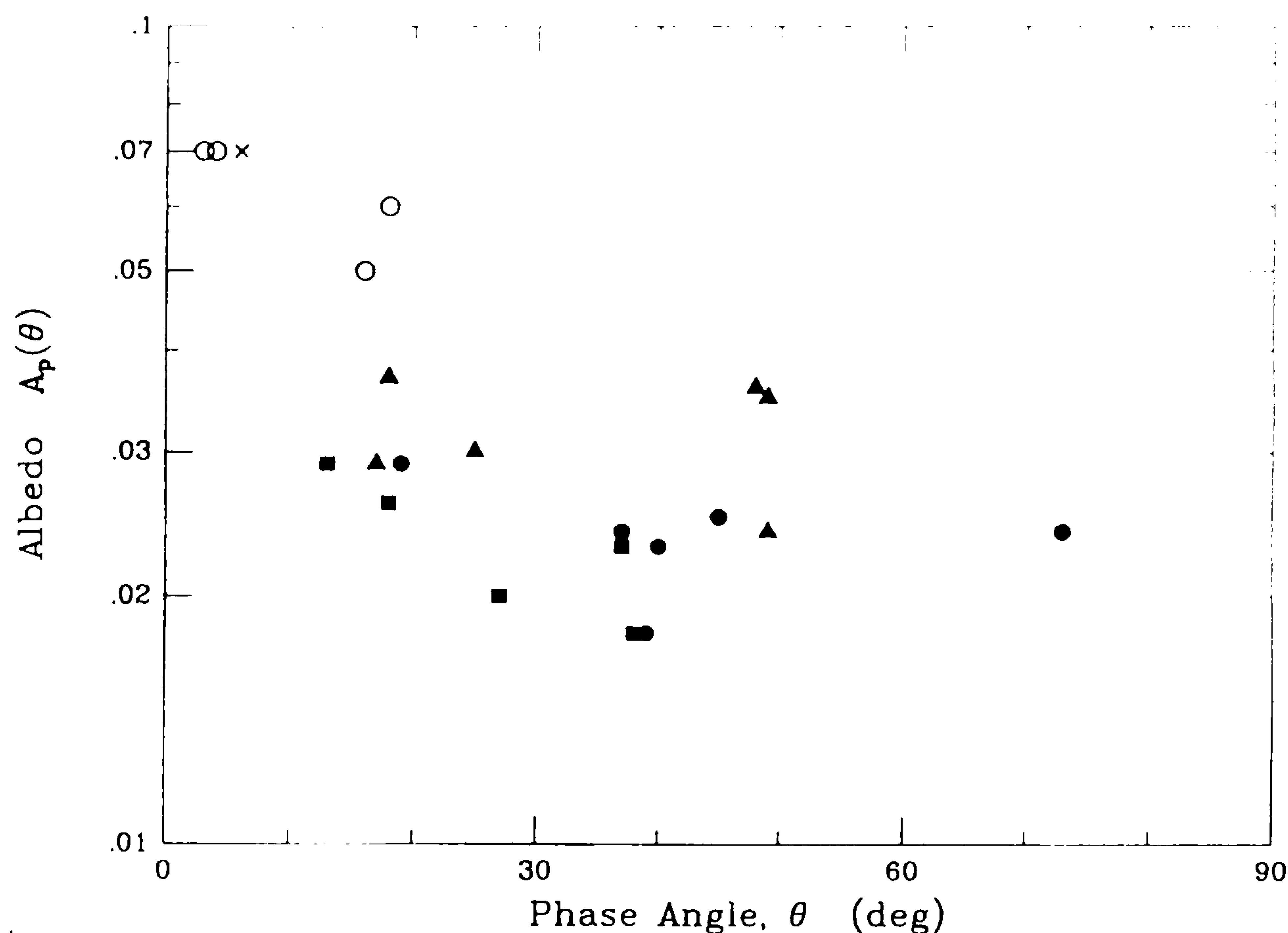


Fig. 3 Mean albedo of comet grains versus phase angle at J(1.25  $\mu\text{m}$ ) (Hanner & Newburn 1989).

## Optical Properties

The optical properties of the dust provide information about the size and structure of the dust particles. While early interpretations were based on Mie theory, strictly valid only for smooth spheres, more recent work emphasizes scattering by irregular particles, as discussed at this Colloquium.

To determine the scattering phase function requires observations over an extended time period as the sun-comet-earth geometry changes. Consequently one has the problem of normalization to account for the changing dust production rate; typically, the gas production rate is used for normalizing the visual continuum, assuming a constant dust/gas ratio. Meech & Jewitt (1987) analyzed the data for 4 comets observed at phase angle  $0^\circ < \theta < 25^\circ$ . They find a linear slope of 0.02 - 0.035 mag/deg. There was no evidence for an opposition surge larger than 20% in P/Halley at  $1.37^\circ < \theta < 8.6^\circ$ . The phase function for the comets from  $0^\circ - 30^\circ$  is steeper than the volume scattering function of zodiacal dust derived by Lamy & Perrin (1986), but less steep than that of dark asteroids. It is consistent with the phase function of fluffy absorbing particles (Hanner *et al.* 1981). Only two comets, West 1976 VI and Bradfield 1980t, have been observed at phase angle  $150^\circ - 120^\circ$  (Ney & Merrill 1976; Ney 1982). The ratio of scattered to thermal energy shows strong forward scattering. The diffraction lobe appears to be wider for the comet dust than for the zodiacal light (Lamy 1985).

The geometric albedo of a particle,  $A_p$ , is defined as the ratio of the energy scattered at  $0^\circ$  phase to that scattered by a white Lambert disk of the same geometric cross section (Hanner *et al.* 1981). Since comets are rarely observed at  $0^\circ$  phase, it is convenient to define the quantity  $A_p(\theta)$  at phase angle  $\theta$ , equal to the geometric albedo times the normalized phase function.



Hanner & Newburn (1989) summarized the  $A_p(\theta)$  at J(1.25  $\mu\text{m}$ ) and K(2.2  $\mu\text{m}$ ) for several comets determined from simultaneous measurements of the scattered and thermal radiation. The albedos are very low, ranging from 0.025 at large phase angle to 0.05 - 0.10 near  $0^\circ$  phase in the J bandpass. Since distant comets tend to be the ones observed near  $0^\circ$ , a systematic bias may be present. Based on a comparison with the  $A_p(\theta)$  derived for P/Halley at  $13^\circ - 18^\circ$ , and with the shape of the phase function in the visible, it does appear that comets beyond 3 AU have higher albedo, a conclusion also reached by Hartman *et al.* (1982), based on the near-infrared colors.

A higher albedo for the dust during times of strong jet activity was seen in comet Halley (Tokunaga *et al.* 1986). This could be due to a shift in the mean grain size or to a component of less-absorbing grains ejected during outburst. Laboratory measurements of the geometric albedo for irregular absorbing particles showed a size dependence from  $A_p \sim 0.08$  for particle radius 2  $\mu\text{m}$  to  $\sim 0.025$  for particle radius 60  $\mu\text{m}$  (Giese *et al.* 1986).

Albedo maps of comets P/Halley (Hammel *et al.* 1987), P/Giacobini-Zinner (Telesco *et al.* 1986), P/Brorsen-Metcalf (Ridgeway *et al.* 1991), and P/Swift-Tuttle (Fomenkova *et al.* 1994) were created by combining CCD images with thermal infrared images. The albedo is not constant across the coma, indicating variation in grain properties. In all 4 cases, the albedo increases radially from the nucleus. The lowest albedo occurs on the anti-sunward side of the nucleus in Halley and Giacobini-Zinner.

The color of the scattered light is generally redder than the sun; the reflectivity gradient decreases with wavelength from 5-18% per 0.1  $\mu\text{m}$  at  $\lambda$  0.35-0.65  $\mu\text{m}$  to 0-2% per 0.1  $\mu\text{m}$  at 1.6-2.2  $\mu\text{m}$  (Jewitt & Meech 1986). The dust is not necessarily the same color as the nucleus. In the case of P/Tempel 2 the J-H color of the nucleus was up to 0.3 mag redder than that of the dust (Tokunaga *et al.* 1992).

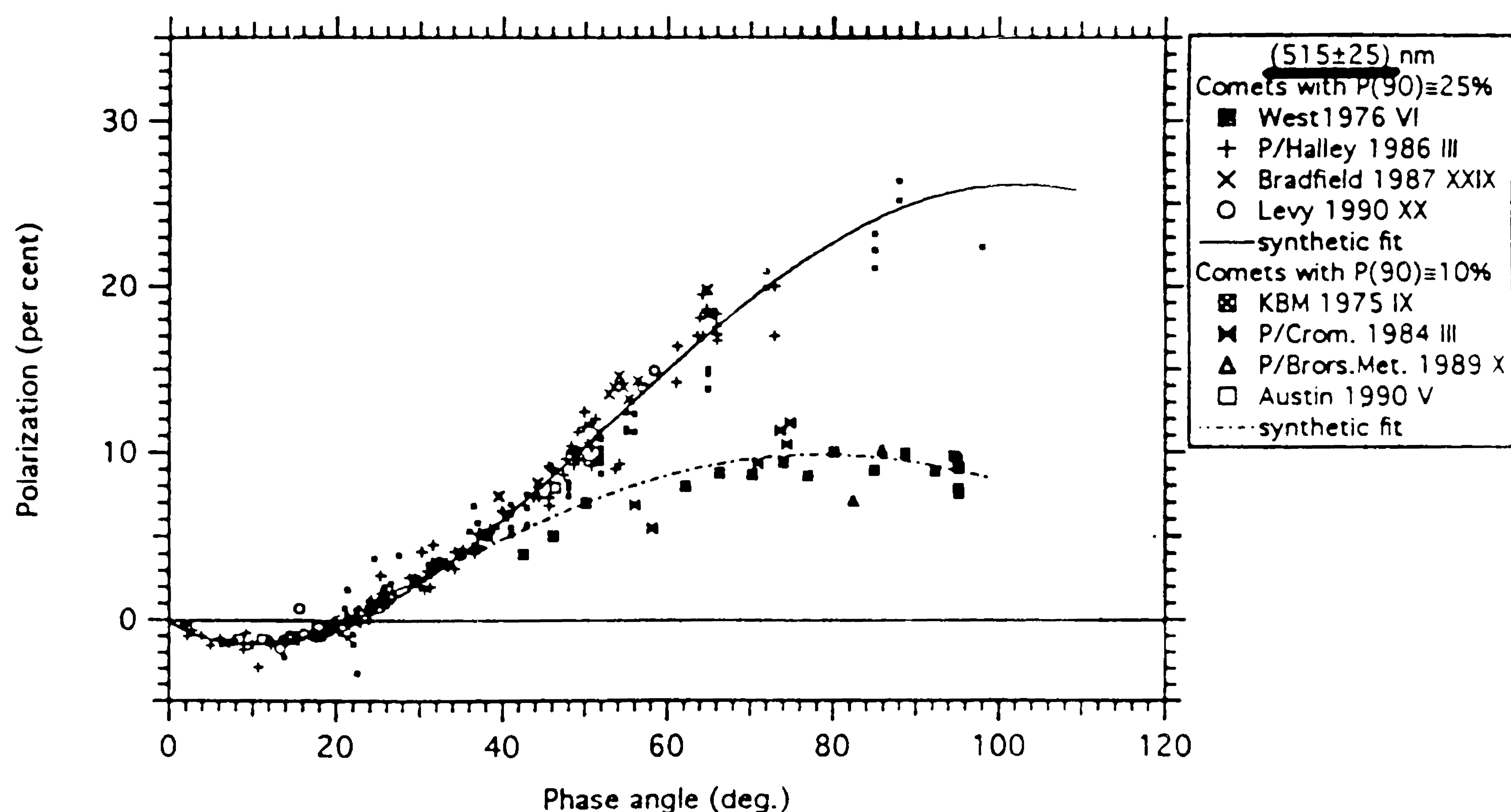


Fig. 4 Polarization versus phase angle at  $\lambda = 0.52 \mu\text{m}$  (Levasseur-Regourd *et al.* 1995)



The polarization phase curve has been measured for a number of comets (Oishi *et al.* 1978; Dollfus *et al.* 1988; Chernova *et al.* 1993; Levasseur-Regourd *et al.* 1995). Polarization has to be observed through filters that isolate the continuum; some earlier measurements were contaminated by gas emission. All of the comets show negative polarization at small phase angles, a neutral point at  $\theta_c = 21 \pm 2^\circ$ , slope  $h \sim 0.2\text{--}0.3\%/ \text{deg}$  at  $\theta_c$ , and maximum polarization near  $90^\circ$ . However, they separate into two groups having  $P_{\text{max}} \sim 10\text{--}15\%$  and  $\sim 25\%$  respectively. The higher  $P_{\text{max}}$  correlates with a stronger dust continuum and stronger silicate emission feature. For sub- $\mu\text{m}$  to  $\mu\text{m}$  particle sizes,  $P_{\text{max}}$  decreases with increasing particle size, as do albedo and silicate emission. Thus, the two groups of comets may have differences in their dust size distribution, although differences in the composition (presence of small "clean" silicates?) or structure (fluffy aggregates?) of the grains could also contribute. In the case of Halley, the polarization at large phase angles increased with wavelength (Dollfus *et al.* 1988), as one would expect if particle size is controlling  $P_{\text{max}}$ .

Spatially resolved observations of the inner coma often show increased polarization in jets (Eaton *et al.* 1988). In their study of polarization in P/Halley, Dollfus *et al.* (1988) distinguish 3 regions: a bright inner halo (radius  $r \sim 100$  km), the inner coma or "fresh" dust ( $r < 5,000$  km) and the outer coma ( $r \sim 10,000$  km). The inner coma consistently produced higher polarization at large phase angles, while the halo displayed lower polarization than the other regions at  $\theta = 30\text{--}40^\circ$ . Lower albedo near the nucleus was also apparent in Halley; both features could be consistent with an excess of larger particles surrounding the nucleus.

## Future Directions

Continuing improvements in ground-based and space-based instrumentation are creating new opportunities for a better understanding of cometary dust.

The sub-arcsec spatial resolution now possible with modern optical and infrared arrays at large ground-based telescopes will allow us to trace the spatial distribution of particles of different size and composition, based on their thermal emission, albedo, color, and polarization. Coordinated infrared, optical, and polarization maps are needed to accomplish this goal. The lower albedo and polarization observed in the near-nucleus region of the coma are not yet satisfactorily explained. Along with these observations, more work on the scattering properties of irregular particles is needed, particularly to understand the polarization.

High resolution  $3 \mu\text{m}$  spectra are required to solve the mystery of the  $3.36 \mu\text{m}$  C-H emission feature and learn more about the  $3.29 \mu\text{m}$  feature. Spectroscopy of comets beyond 3 AU may detect icy grains, particularly the  $3 \mu\text{m}$  water ice feature, as well as volatile organic species.

The origin of the crystalline olivine grains remains a puzzle. So far, the  $11.2 \mu\text{m}$  olivine feature has been seen in only 4 comets and we need to understand why it appears in some comets and not others.

More sensitive submillimeter detectors will allow detection of thermal emission,



or useful upper limits, to constrain the abundance of large particles in the coma. This is important for determining the total rate of mass loss from the nucleus.

The ISO satellite will make infrared photometric, spectroscopic, and imaging observations of several comets in the next 18 months. The entire infrared spectrum from 3 - 200  $\mu\text{m}$  will be accessible. We can expect new insights from these observations.

**Acknowledgements.** This research was performed at the Jet Propulsion Laboratory, California Institute of Technology, under contract with the National Aeronautics and Space Administration.

## References

- Baas, F., Geballe, T. R. and Walther, D. M. 1986, *ApJ Lett.* 311, L97  
 Bockelée-Morvan, D., Brooke, T. Y. and Crovisier, J. 1995, *Icarus* 116, 18  
 Bradley, J. P. 1994, *Science* 265, 925  
 Bradley, J. P. 1995, this volume  
 Bregman, J. et al. 1987, *A&A* 187, 616  
 Brooke, T. Y., Tokunaga, A. T. and Knacke, R. F. 1991, *AJ* 101, 268  
 Brownlee, D. 1995, these proceedings  
 Campbell, D. B., Harmon, J. K. and Shapiro, I. I. 1989, *ApJ* 338, 1094  
 Campins, H. and Ryan, E. 1989, *ApJ* 341, 1059  
 Chernova, G. P., Kiselev, N. N. and Jockers, K. 1993, *Icarus* 103, 144  
 Clemett, S. J., Maechling, C. R., Zare, R. N., Swan, P. D. and Walker, R. M. 1993, *Science* 262, 721  
 Combes, M. et al. 1988, *Icarus* 76, 404  
 Davies, J. K., Green, S. F. and Geballe, T. R. 1991, *MNRAS* 251, 148  
 Di Santi, M. A., Mumma, M. J., Geballe, T. R. and Davies, J. K. 1995, *Icarus* 116, 18  
 Dollfus, A., Bastien, P., Le Borgne, J.-F., Lévassieur-Regourd, A. C. and Mukai, T. 1988, *A&A* 206, 348  
 Duncan, M., Quinn, T. and Tremaine, S. 1988, *ApJ Lett.* 328, L69  
 Eaton, N., Scarrott, S. M. and Warren-Smith, R. F. 1988, *Icarus* 76, 270  
 Fomenkova, M., Larson, S., Jones, B. and Pina, R. 1994, *Bull. AAS* 26, 1119  
 Giese, R. H., Killinger, R. T., Kneissel, B. and Zerull, R. H. 1986, *ESA SP-250*, II, p. 53  
 Goldstein, R. M., Jurgens, R. F. and Sekanina, Z. 1984, *AJ* 89, 1745  
 Hammel, H. B., Telesco, C. M., Campins, H., Decher, R., Storrs, A. D. and Cruikshank, D. P. 1987, *A&A* 187, 665  
 Hanner, M. S. 1983, in *Cometary Exploration*, ed. T. I. Gombosi, II, 1  
 Hanner, M. S. et al. 1985, *Icarus* 64, 11  
 Hanner, M. S. and Newburn, R. L. 1989, *AJ* 97, 254  
 Hanner, M. S., Giese, R. H., Weiss, K. and Zerull, R. 1981, *A&A* 104, 42  
 Hanner, M. S., Hackwell, J. A., Russell, R. W. and Lynch, D. K. 1994b, *Icarus* 112, 490  
 Hanner, M. S., Lynch, D. K. and Russell, R. W. 1994a, *ApJ* 425, 274  
 Hanner, M. S., Newburn, R. L., Gehrz, R. D., Harrison, T., Ney, E. P. and Hayward, T.



- L. 1990, *ApJ* 348, 312
- Harmon, J. K., Campbell, D. B., Hine, A. A., Shapiro, I. I. and Marsden, B. G. 1989, *ApJ* 338, 1071
- Hartmann, W. K., Cruikshank, D. P., and Degewij, J. 1982, *Icarus* 52, 377
- Hoban, S., Mumma, M. J., Reuter, D. C., Di Santi, M. A., Joyce, R. R. and Storrs, A. 1991, *Icarus* 93, 122
- Jessberger, E. K., Christoforidis, A. and Kissel, J. 1988, *Nature* 332, 691
- Jewitt, D. C. and Luu, J. X. 1995, *AJ* 109, 1867
- Jewitt, D. C. and Luu, J. X. 1992, *Icarus* 100, 187
- Jewitt, D. C. and Luu, J. X. 1990, *ApJ* 365, 738
- Jewitt, D. C. and Meech, K. J. 1986, *ApJ* 310, 937
- Kissel, J. et al. 1986, *Nature*, 321, 280, and 336
- Lamy, Ph. L. 1985, in *Asteroids, Comets, Meteors II*, ed. Lagerkvist et al. 373
- Lamy, Ph. L. and Perrin, J.-M. 1986, *A&A* 163, 269
- Levasseur-Regourd, A. C., Dumont, R., Goidet-Devel, B., Hadamcik, E., Renard, J. B. 1995, in preparation.
- Lynch, D. K. et al. 1989, *Icarus* 82, 379
- Lynch, D. K., Hanner, M. S., and Russell, R. W. 1992a, *Icarus* 97, 269
- Lynch, D. K., Russell, R. W., Hackwell, J. A., Hanner, M. S. and Hammel, H. B., 1992b, *Icarus* 100, 197
- Meech, K. J. and Jewitt, D. C. 1987, *A&A* 187, 585
- McDonnell, J.A.M., Lamy, P. L. and Pankiewicz, G. S. 1991, in *Comets in the Post-Halley Era*, ed. R. L. Newburn, M. Neugebauer, and J. Rahe, Kluwer Dordrecht, 1043.
- Ney, E. P. 1982, in *Comets*, ed. L. L. Wilkening, p. 323
- Ney, E. P. and Merrill, K. M. 1976, *Science* 194, 1051
- Oishi, M., Kawara, K., Kobayashi, Y., Maihara, T. Noguchi, K., Okuda, H. and Sato, S. 1978, *Pub. Astron. Soc. Japan* 30, 149
- Ridgeway, S. E. Jewitt, D., Campins, H., Luu, J., Joy, M., Sisk, C., and Telesco, C. M. 1991, in *Astrophysics with Infrared Arrays*, ASP Conf. Ser. 14, 329
- Reuter, D. C. 1992, *ApJ* 386, 330
- Stephens, J. R. and Russell, R. W. 1979, *ApJ* 228, 780
- Telesco, C. M. et al. 1986, *ApJ. Lett.* 310, L61
- Tokunaga, A. T., Golisch, W. F., Griep, D. M., Kaminski, C. D. and Hanner, M. S. 1986, *AJ* 92, 1183
- Tokunaga, A. T., Hanner, M. S., Golisch, W. F., Griep, D. M., Kaminski, C. D. and Chen, H. 1992, *AJ* 104, 1611
- Xing, Z. and Hanner, M. S. 1995, this volume